

Videogrammetry methods in experimental aerodynamics

Vladimir Kulesh

Central Aerohydrodynamic Institute named after prof. N.E. Zhukovsky (FSUE «TsAGI»),
Zhukovsky, Moscow Region, Russia
mera@tsagi.ru

Abstract The videogrammetry method with using one digital camera only was chosen as a mainstream of non-contact measurements of the distributed parameters of movements and deformations of the objects under test in aerodynamic experiments at TsAGI. More than twenty years' experience showed the advantages of this concept in difficult conditions of limited visual field and bounded work space in wind tunnels and experimental facilities. It is proposed to formulate prior information in the form of mathematical parametric hypothesis and complement the system of equations of the operating characteristics by it. The measurements of bend and twist deformation of the wings, elastic deformations of the "smart" adaptive leading-edge flap and deformations of the rotation machine elements are presented as examples of this method in different applications at TsAGI. It is shown in practice that, in the conditions of aerodynamic experiment measurement error is about 0.1 mm and twisting deformation errors amounts in the range of 0.01 to 0.1 degrees.

Keywords: videogrammetry, digital camera, deformation measurements, optical measurements

1 Introduction

Videogrammetry (VGM) is a development of the traditional photogrammetry method. It is based on the use of modern methods and means of digital recording and numerical analysis of images. Videogrammetry appeared in the early 90s with the appearance of compact digital cameras with solid state photosensitive elements CCD matrixes.

The essence of the method is following: one can find 3 spatial coordinates x, y, z of object point knowing only 2 response coordinates u, v in the digital image, which are obtained according to the laws of the central projection (Fig. 1). In the general formulation, this problem underdetermined there are three unknowns and only two equations. There are three ways to solve this problem of uncertainty coordinates recovering.

The first way is a stereometry, where two or more images of the same object are received from different positions. Solution of a problem is reduced to combination of equations obtained from different images. This is a traditional and universal way.

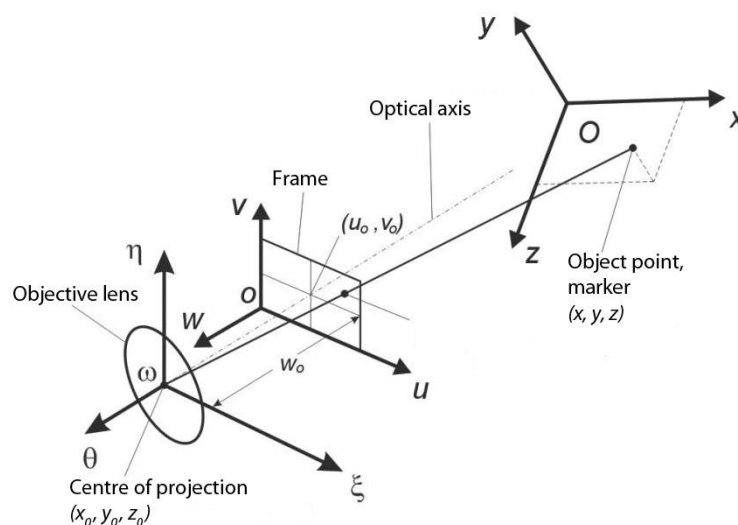


Fig. 1 Image foundation by digital camera objective lens

Another approach is application of structured illumination, where the missing information is obtained from the known trajectories of illuminating rays. In this case, most commonly, a cross-section light plane or a collimated beam of light rays are applied.

The third way is the use of apriori known information obtained from other sources.

2 Basic concept

Experiment in wind tunnels and on the stands is usually accompanied with severe space restrictions on equipment location and optical access to the object of research. Therefore, the first two ways of solving the problem of the uncertainty coordinates recovering is rarely used. The vast majority of practical problems are solved by the third way, which realization requires only one digital camera.

In this way, there are two approaches: direct and inverse. Using the direct approach, operating characteristic of the measuring system can be written as a direct system of equations

$$\begin{cases} x = x_0 + (z - z_0) \frac{M_{11} \cdot (u - u_0) + M_{12} \cdot (v - v_0) + M_{13} \cdot w_0}{M_{31} \cdot (u - u_0) + M_{32} \cdot (v - v_0) + M_{33} \cdot w_0} \\ y = y_0 + (z - z_0) \frac{M_{21} \cdot (u - u_0) + M_{22} \cdot (v - v_0) + M_{23} \cdot w_0}{M_{31} \cdot (u - u_0) + M_{32} \cdot (v - v_0) + M_{33} \cdot w_0} \end{cases} \quad (1)$$

Prior information is reduced to the establishment of an explicit dependence between one coordinate, for example z , from two others. This dependence is added to the system of equations (1) that provides a solution to the problem of coordinates recovering.

Using inverse approach, operating characteristic of the measuring system is represented in the reverse form

$$\begin{cases} u = w_0 \frac{M'_{11}(x - x_0) + M'_{12}(y - y_0) + M'_{13}(z - z_0)}{M'_{31}(x - x_0) + M'_{32}(y - y_0) + M'_{33}(z - z_0)} + u_0; \\ v = w_0 \frac{M'_{21}(x - x_0) + M'_{22}(y - y_0) + M'_{23}(z - z_0)}{M'_{31}(x - x_0) + M'_{32}(y - y_0) + M'_{33}(z - z_0)} + v_0; \end{cases} \quad (2)$$

Prior information is given in the form of coordinates of group of points on the investigated object surface in original undeformed state. Based on the presumable law, parametric hypothesis of motion and deformation is created. The R parameters of the hypothesis are varied, forecast for point coordinates in image is calculated using equations (2) and the inverse problem regarding the parameters of motion and deformation is solved.

3 Coefficients of operating characteristic

Operating characteristic of the measuring system (1) and (2) depends on the group of coefficients, such as: x_0, y_0, z_0 the projection center o in the object coordinate system; u_0, v_0, w_0 coordinates of the image principal point; M_{ij} ($i, j = 1, 2, 3$) – the matrix elements of the direction cosines of the camera coordinate system in the object coordinate system

$$M = \begin{pmatrix} M_{11} & M_{12} & M_{13} \\ M_{21} & M_{22} & M_{23} \\ M_{31} & M_{32} & M_{33} \end{pmatrix}$$

In aerodynamic experiment it is common to represent the matrix M through successive rotation of aerodynamic model first on the course angle β around vertical Oy axis, then on the tangage angle α around Oz axis in a rotated coordinate system, and finally on a roll angle γ around Ox axis. As a result, the matrix of the directional cosines takes the form

$$M(\alpha, \beta, \gamma) = \begin{pmatrix} \cos \beta \cdot \cos \alpha & \sin \beta \cdot \sin \gamma - \sin \alpha \cdot \cos \beta \cdot \cos \gamma & \sin \beta \cdot \cos \gamma + \sin \alpha \cdot \cos \beta \cdot \sin \gamma \\ \sin \alpha & \cos \alpha \cdot \cos \gamma & -\cos \alpha \cdot \sin \gamma \\ -\cos \alpha \cdot \sin \beta & \cos \beta \cdot \sin \gamma + \sin \alpha \cdot \sin \beta \cdot \cos \gamma & \cos \beta \cdot \cos \gamma - \sin \alpha \cdot \sin \beta \cdot \sin \gamma \end{pmatrix}$$

In special cases, the order of the model rotation may be different, but numerical values of the rotation matrix elements will remain unchanged.

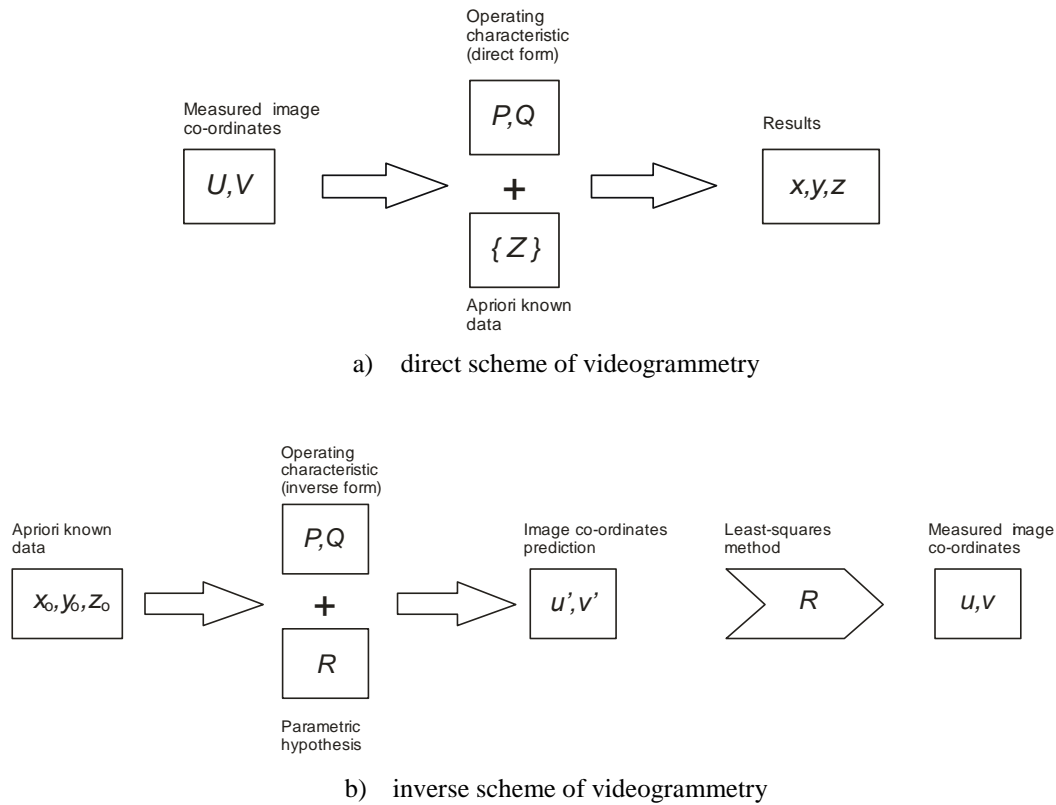


Fig. 2 Schemes for solving the problem of the coordinates recovering

The majority of real receiving objective lenses make a significant geometric distortion that must be considered in image processing. Usually, standard objective lenses have most influential noise called «distortion» the noise which is symmetric with respect to the optical axis. Distortion can be described by even power polynomial of the radius $r = \sqrt{(u - u_0)^2 + (v - v_0)^2}$. In the first approximation, the objective lens distortion can be amended by corrections of the second order

$$u' \approx u_0 + (u - u_0) \cdot \left(1 - \frac{d}{w_0} \cdot r^2 \right),$$

$$v' \approx v_0 + (v - v_0) \cdot \left(1 - \frac{d}{w_0} \cdot r^2 \right),$$

where the dimensionless coefficient d is called the coefficient of the objective lens distortion.

Terms of higher degree of the distortion polynomial and non-axisymmetric distortions occur less frequently, but if it is necessary, they can be taken into account as additional corrections. Six coefficients of the operating characteristic $P = (x_0 \ y_0 \ z_0 \ \alpha \ \beta \ \gamma)$ are referred to as exterior orientation parameters in photogrammetry, and the rest $Q = (u_0 \ v_0 \ w_0 \ d \ \dots)$ – interior orientation parameters. Formally geometric distortion parameters of the image are supplemented by interior orientation parameters.

4 Calibration of measurement system

While calibration of measurement system in space of experiment one should define (in some way) an array of grid points with known coordinates x^*, y^*, z^* , register one or more images and find the coordinates u^*, v^* of centers of corresponding points in the pictures. Then, by means of mathematical comparison of array x^*, y^*, z^* with an array u^*, v^* using regression procedures, unknown coefficients values of measuring system operating characteristic are obtained.

An array of grid points in space is given by the special calibration test-objects (calibration rig) with markers, which location geometric characteristics are previously accurately measured with precision tools [1]. Test-object spatial position in the object coordinate system is achieved by using auxiliary measuring tools.

Typically, calibration is carried out in two stages. In the first stage the parameters of interior orientation are determined. This should be carried out as accurately as possible, so it is carried out under well-controlled laboratory conditions. In this procedure, it is advisable to apply a test-object, which has a large number of markers, more fully and evenly covering the entire image frame.

The second step is carried out just on the place of location of measurement system: on experimental setup or in wind tunnel. At this stage, the exterior orientation parameters are obtained, thus the camera coordinate system is connected with the object coordinate system.

5 Application of VGM method

In aerodynamic experiment methods using prior information are successfully applied to the measurement of geometrical shape parameters, motion paths and pattern deformations of aircraft structural elements, full-scale blades of helicopter main rotor, propeller and prop fan blades in wind tunnels and stand tests [2-3]. Wherein, the marker point method is applied. VGM methods allow solving such actual problems of experimental aerodynamics, as

- slackness problem of "stiff" models;
- measurement and updating of the model location in the wind tunnel flow;
- behavior investigation and verification of the theoretical and elastic models;
- investigation of motion and deformation of the rotating machines;
- study of the motion trajectories of free-flying models.

6 Deformation measurements of the model

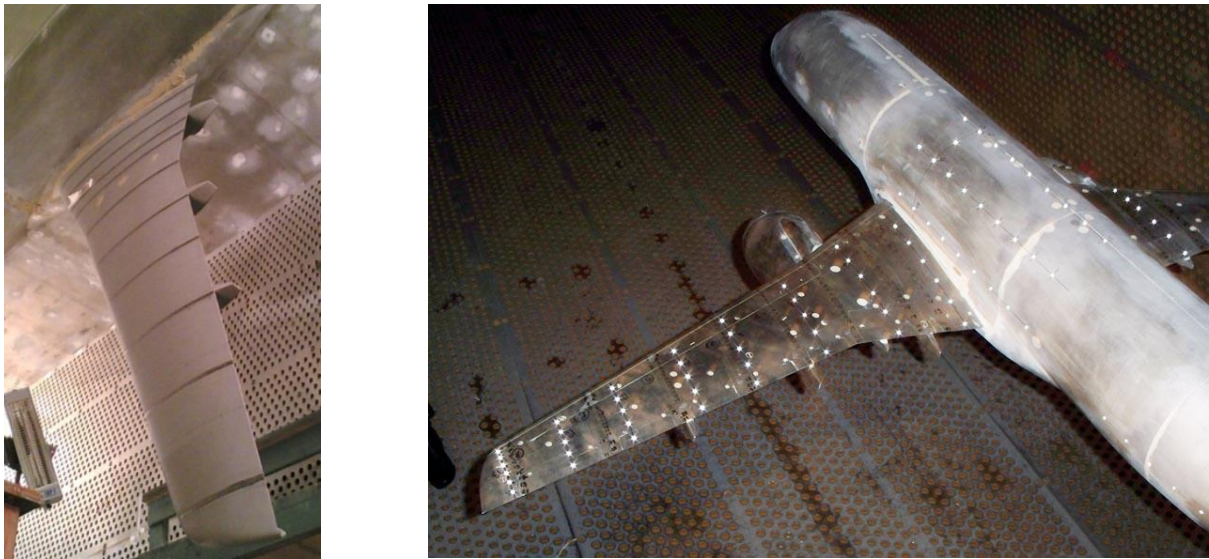
The measurements of deformation of a model in a wind tunnel flow are regularly carried out in TsAGI's wind tunnels T-101, T-103, T-104, T-107, T-128 et al., since 1994 [2,3]. Usually the most interesting are bearing elements: wing, stabilizer fin and others. They are characterized by large elongation. To measure the bending and twist deformations of these elements the direct scheme for solving the problem of coordinate recovering is applied. As apriori hypothesis one should apply the known values of the longitudinal coordinate, neglecting its small changes $z = z^* = \text{const}$. If z coordinate cannot be considered as constant under large bending deformation, the corrections may be required.

Fig. 3 shows the examples of studies of deformation of rigid and elastic models of aircraft in transonic and subsonic wind tunnels. Fig. 4 represents typical examples of bending and twist deformations of aircraft wing model. Measurement error of linear deviations depends on the external experiment conditions and is estimated at about 0.1 mm/m.

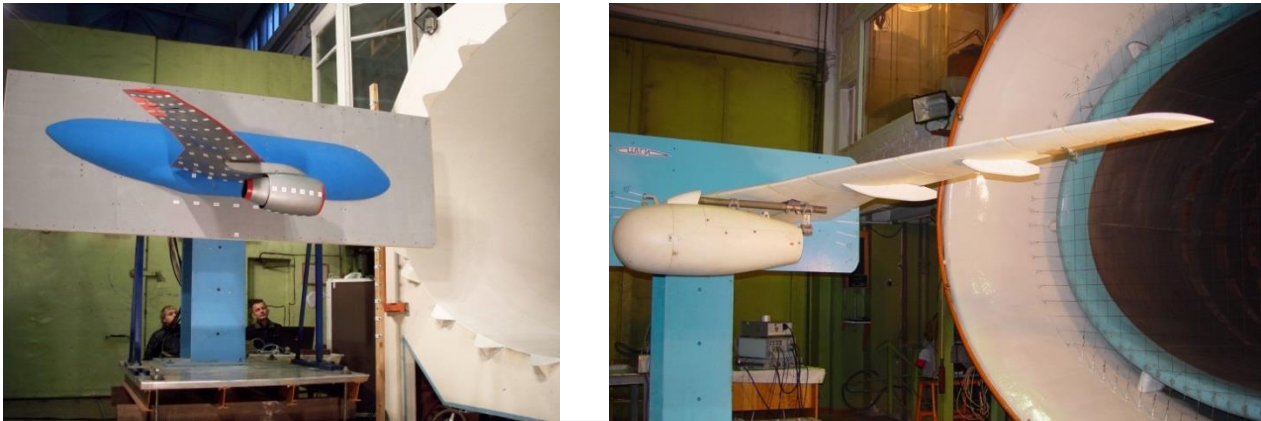
7 Deformation measurements of adaptive nose part of a wing

The method will be considered in detail at the example of non-contact elastic deformation measurements of the demonstrator-wing with adaptive "smart" nose part [3]. These measurements were carried out in a large wind tunnel T-101 in TsAGI in according with SADE international project of 7th European Framework Program in 2012. The photo of the experimental setup is shown in Fig. 5a, a diagram of demonstrator-wing - in Fig. 5 b. The constituent parts of the demonstrator were flexible adaptive nose part (leading edge) 1, wing body (central power part of the wing) 2 and wing trailing-edge flap 3. Two flow shutters 4 were established on the tips of the demonstrator-wing model. The demonstrator was installed on the racks of the aerodynamic balance 6, which are above control cabin 7. The nose part had a width of 650 mm along the chord and consisted of three separate sections along the model span. The first one had a length of 2 m in the middle of the wing and the others were 1.5 m at the ends.

For simultaneous deformation measurements of the upper and lower surfaces of the large-scale aerodynamic model dual-channel videogrammetry system was developed. The system consists of two digital cameras 1, placed in the left flow shutter of the demonstrator (Fig. 6a). Cameras had matrix resolution of 1392×1040 pixels and objective lenses with focal length of 16 mm. The image transfer from both cameras was carried out via Ethernet channel.



a) study of rigid models in transonic wind tunnel T-128



b) study of elastic wing models in subsonic wind tunnel T-103

Fig. 3 Examples of deformation measurements of wings in wind tunnels flow

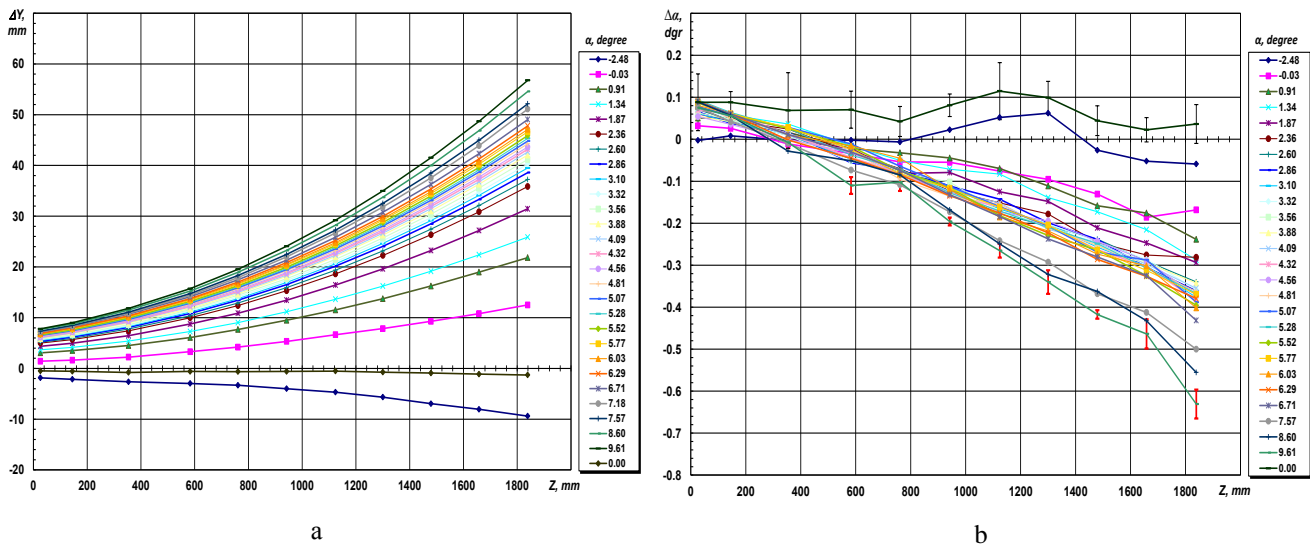
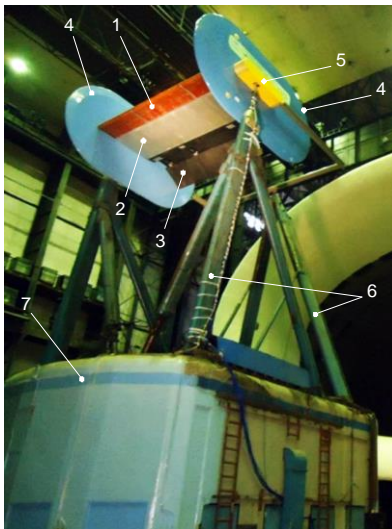
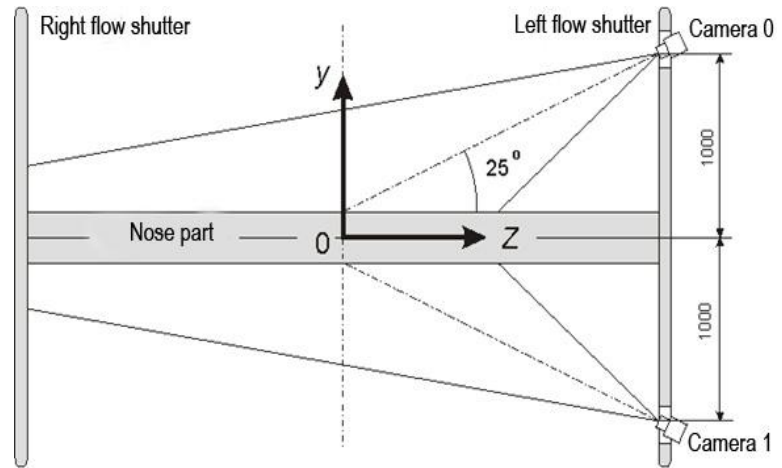


Fig. 4 Typical measurement results of bending(a) and twist(b) deformation of the wing



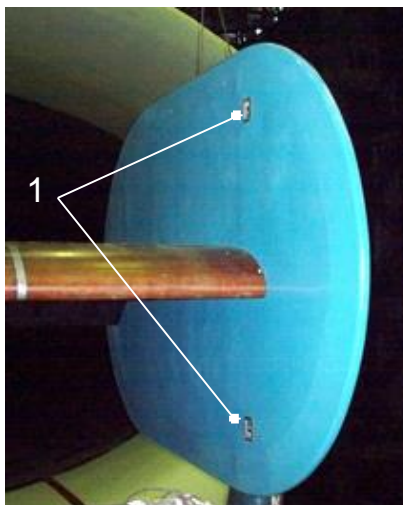
a) experimental setup



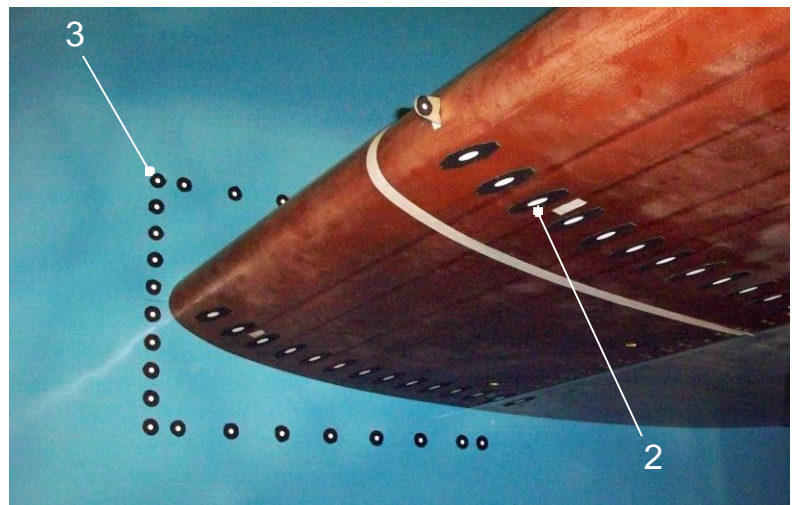
b) diagram of demonstrator-wing

Fig. 5 Investigation of elastic deformations of adaptive “smart” nose wing part

The origin of coordinate system was placed at the point of the wing chord on the front wing body cut in the vertical plane of symmetry of the model. Ox axis was directed along the chord in the stream direction, Oy axis – upwards, perpendicular to the chord, and Oz axis – along the span to the direction of cameras. Three interconnected systems of markers were applied on the model surface (Fig. 6b). Two measuring systems of markers were located on the top and bottom surfaces of the nose part within ten sections with values of z coordinate 1300, 1050, 950, 475, 0, 475, 950, 1050, 1600 and 2480 mm. Each section contained 14 markers. The first marker was located on the wing box at point $x = 25$ mm and following ones – along the profile arc to the nose with 50 mm step. Markers had an elliptical shape. Their sizes (along minor axis from 3 to 9 mm) and orientation were calculated so that markers in the images would have the form of circle with a diameter about 5 pixels. The reference system of markers included two lines of markers: first line consisted of markers that were already on the top and bottom of the wing box at points with x coordinate 25 mm, and another one included a group of additional markers placed on the surface of opposite (right) flow shutter visible by the two cameras. Coordinates of all markers were measured with manual measuring instrument. Standard lighting system of the test section of the wind tunnel served as a source of continuous illumination for the wing surface.



a) two cameras in left shutter



b) markers on the nose and right shutter

Fig. 6 Location diagram of digital cameras 1 and markers 2,3

Calibration of the measurement system was carried out in 2 stages. The first stage allowed estimating the instrumental measurement error by two coordinates being ± 0.2 mm. The second stage consists of definition of the current values of exterior orientation parameters of the operation characteristic for each registered working frame by the group of reference markers located on the wing box and opposite right flow shutter. This made it possible to eliminate the influence of uncontrolled shifts of cameras resulting from general deformation of the model.

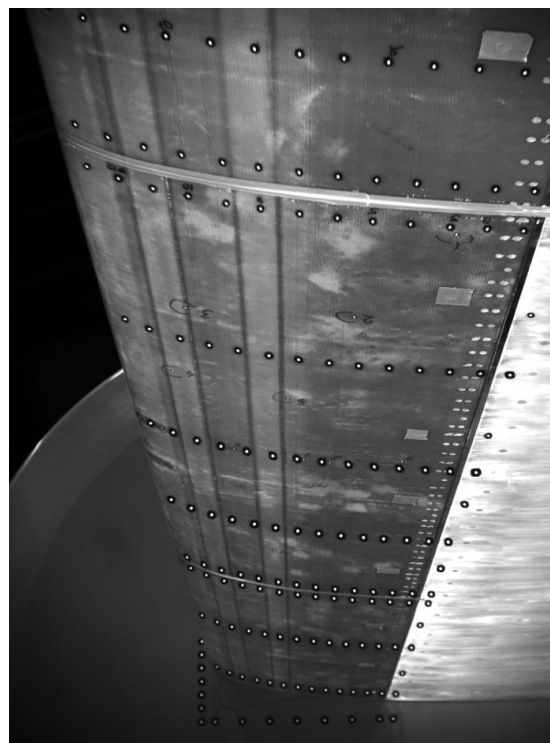
Measurement was conducted with a nose in a deflected position (takeoff and landing) and undeflected position (cruising mode). In each case measurements of x, y coordinates for all markers on angles of attack of 10, 5, 0, 5, 10, 15, 19 and 22 degrees were carried out. Measurements of coordinates of "undeformed" model markers for all angles of attack without flow in the wind tunnel and then at the same angles at flow velocity of 30, 40 and 50 m/s were preliminary made. Examples of the work images of top and bottom nose surfaces are shown in Fig. 7.

Images processing was performed using a set of standard and special programs. While processing the following steps were performed: measurement of u,v coordinates of marker projection centers on each image; calculation of x,y coordinates of corresponding points on the surface, according to the formulas of the perform characteristic (1); finding deformation parameters by subtracting the coordinates of points on the surface in a "wind-off" state from the coordinates in the current "wind-on" state.

The results of measurements of the nose profile shape in deflected and undeflected states without a flow are shown in Fig. 8. Fig. 9 represents an example of three-dimensional visualization of deflection fields along the axis Oy of upper and lower surfaces in the most deformed state in the test mode with undeflected nose on angle of attack of 22° and flow velocity of 50 m/s. The maximum deviation along Oy axis was up to 5 mm in the nose area on the bottom surface of the middle section of the adaptive nose part. Longitudinal wavy variations of vertical deviations of the surface, which correlate with the configuration of structure supporting the skin, were observed in all modes. Formation of ledges at the joints of adjacent sections of nose wing part, reaching maximum values of 1 mm on the lower surface on the right junction and 1.5 mm on the left, was also observed.



a) top camera view



b) bottom camera view

Fig. 7 Work images from 2 cameras

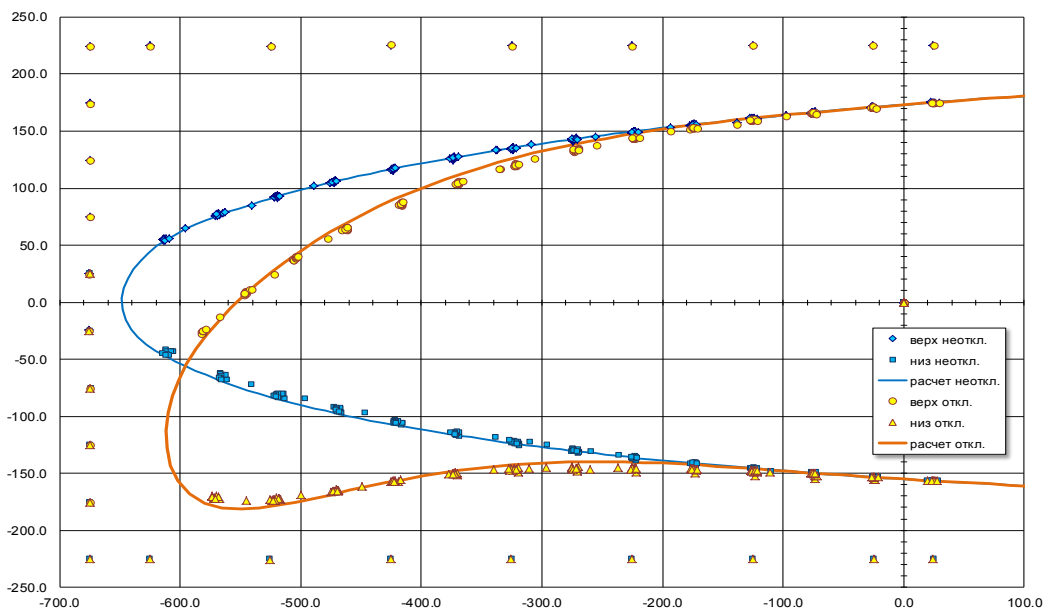


Fig. 8 The results of measurements of the nose shape in deflected and undeflected states (in millimeters)

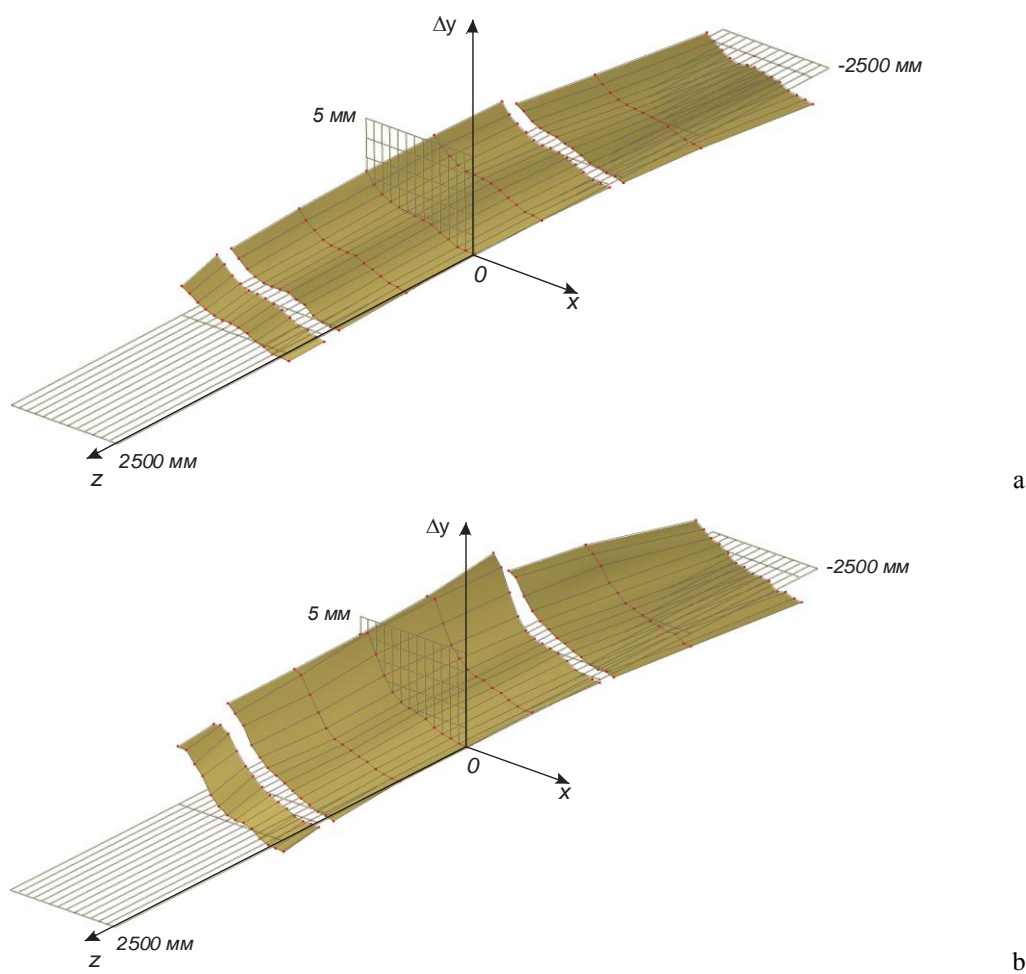


Fig. 9 Three-dimensional presentation of deformation fields of top (a) and bottom (b) surfaces of nose

8 Deformation measurements of rotating objects

A large group of problems of aerodynamic experiment is related to studies of characteristics of rotating objects, such as propeller blades and helicopter main rotor. These elements perform complex motion in space, including a circular motion in the plane of rotor rotation, flapping in the plane perpendicular to the plane of rotation, rotational motion associated with propeller pitch control and moreover they are subjected to bending and twist deformation.

Studies of motion and deformation of full-scale main rotor blades by VGM method are carried out in the T-101, T-104 wind tunnels and at TsAGI's hovering since 1996 (Fig. 10) [4-6]. The dimensions of the experimental setup made it possible to establish a digital recording camera on the hub of the rotor, so that its field of view constantly contained the researched blade with applied markers located in 10-12 specified sections. In this case, the measurements were performed in rotating coordinate system, and it was possible to apply the direct videogrammetry scheme (1) and a parametric model $z = z^* = \text{const}$ (Oz axis is directed along the longitudinal axis of the blade). Measurement error of linear deviation of the sections at the tip of the blade with radius of 6.5 m was estimated no more than 0.5 mm, while angular deviation was 0.1 degrees. The scope of deformation studies of rotating objects continued its development with the VGM method to measure static deformation of coaxial open rotor blades that was proposed in according with DREAM international project of 7th European Framework Program in 2009. The diameter of rotors was approximately 600 mm and the length of blades was about 190 mm. The dimensions of the rotor in this case didn't allow to locate camera on the axis of rotation - it was fixedly mounted at a distance of about 1.5 m. Camera field of view simultaneously contained only one blade of each of two rotors. Synchronization of camera was performed by each rotor in turn. Lighting of blades was carried out by means of a gas discharge flash-lamp with pulse duration of about 3 microseconds.

Fig. 11 represents the location of the measuring equipment close to the rotor, and Fig. 12 - the working image, synchronized by the second rotor blade (at the top of frame).

In this case parametric hypothesis $z = z^* = \text{const}$ was supplemented with the assumption that the deformation of the blade in the plane of maximum stiffness Oxz is negligible $\Delta x = 0$. This allowed to separate small deviations due to deformation from the large ones due to the rotation of the rotor.

Measurements of instantaneous static deformation were carried out at external flow Mach numbers from $M = 0.2$ in subsonic T-104 wind tunnel to $M = 0.76$ in transonic T-107 wind tunnel in TsAGI with rotor rate up to 8500 rpm. Measurement error of linear deviations due to deformation was estimated as 0.1 mm and angular deviations of blade sections due to twist – 0.05 0.1 degrees.



Fig. 10 Measurements of motion and deformation parameters of helicopter rotor blades on the hovering (a) and in the T-101 wind tunnel (b)

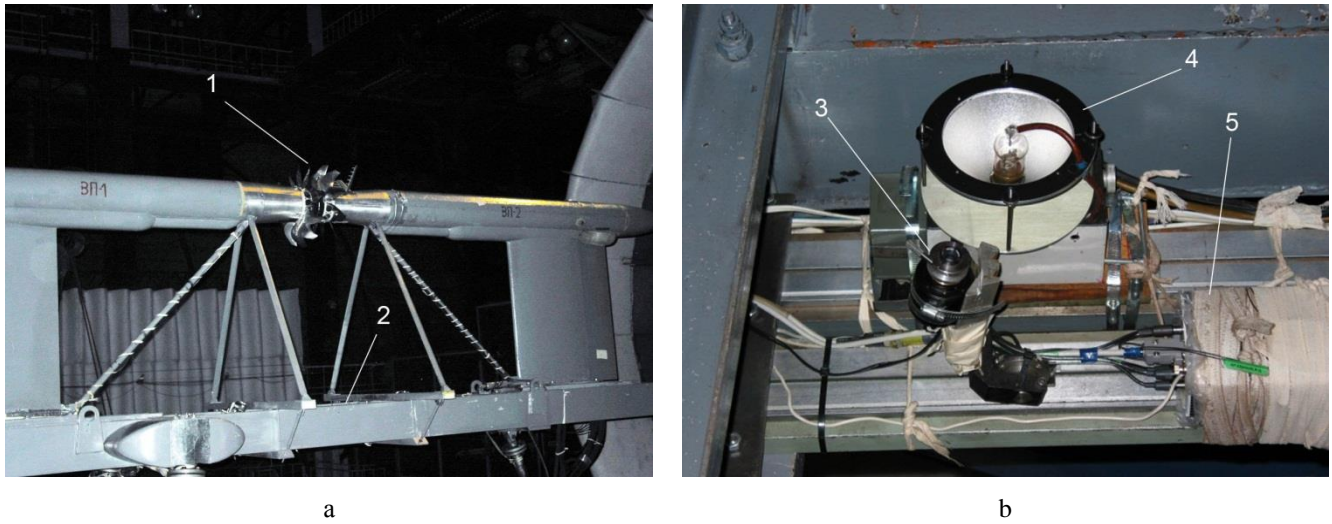


Fig. 11 Experimental setup (a) and location of the optical equipment on it (b): 1-investigated rotor 2-location of the optical system 3-digital camera 4-flash-lamp, 5-block of synchronization

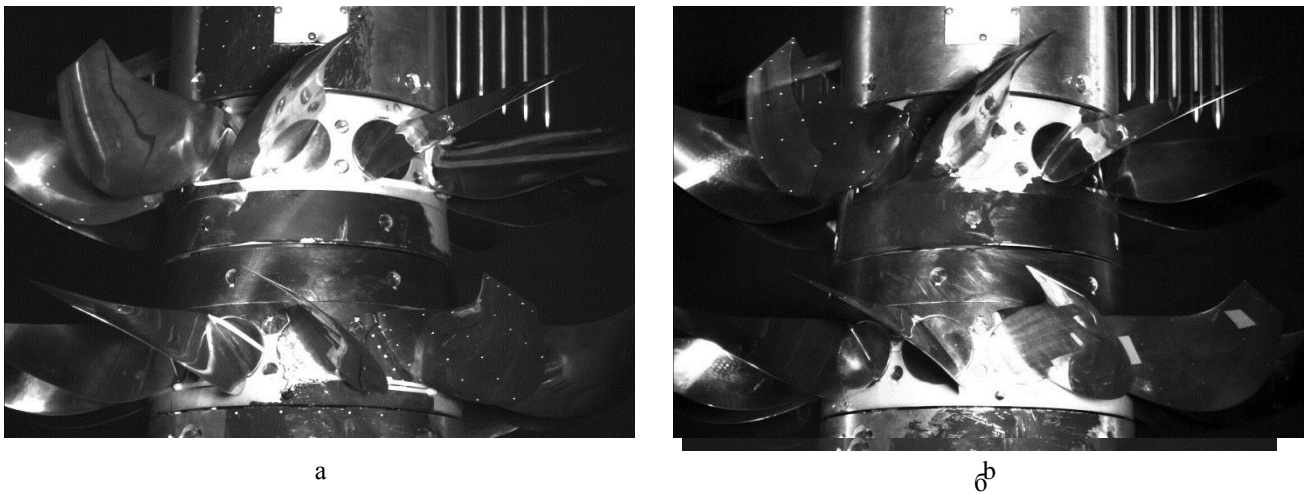


Fig. 12 Working images obtained by synchronization with front (a) and the rear blade(b)

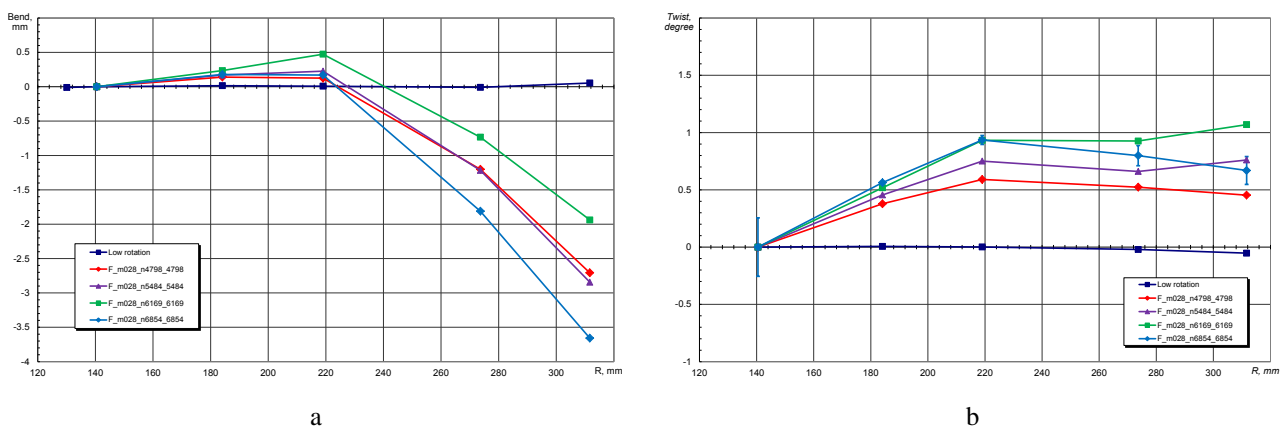


Fig. 13 Measurement results of bending (a) and twist (b) deformation of the front blade at $M = 0.28$, and rotor rate of $n = 4798$ to 6854 rpm

The most difficult implementation of VGM method was measurements of motion and deformation parameters of blades of helicopter rotor model with a diameter of about 5 m in T-104 wind tunnel. Photos of the experimental setup, the measurement diagram and the view of blades with applied markers are shown in Fig. 14.

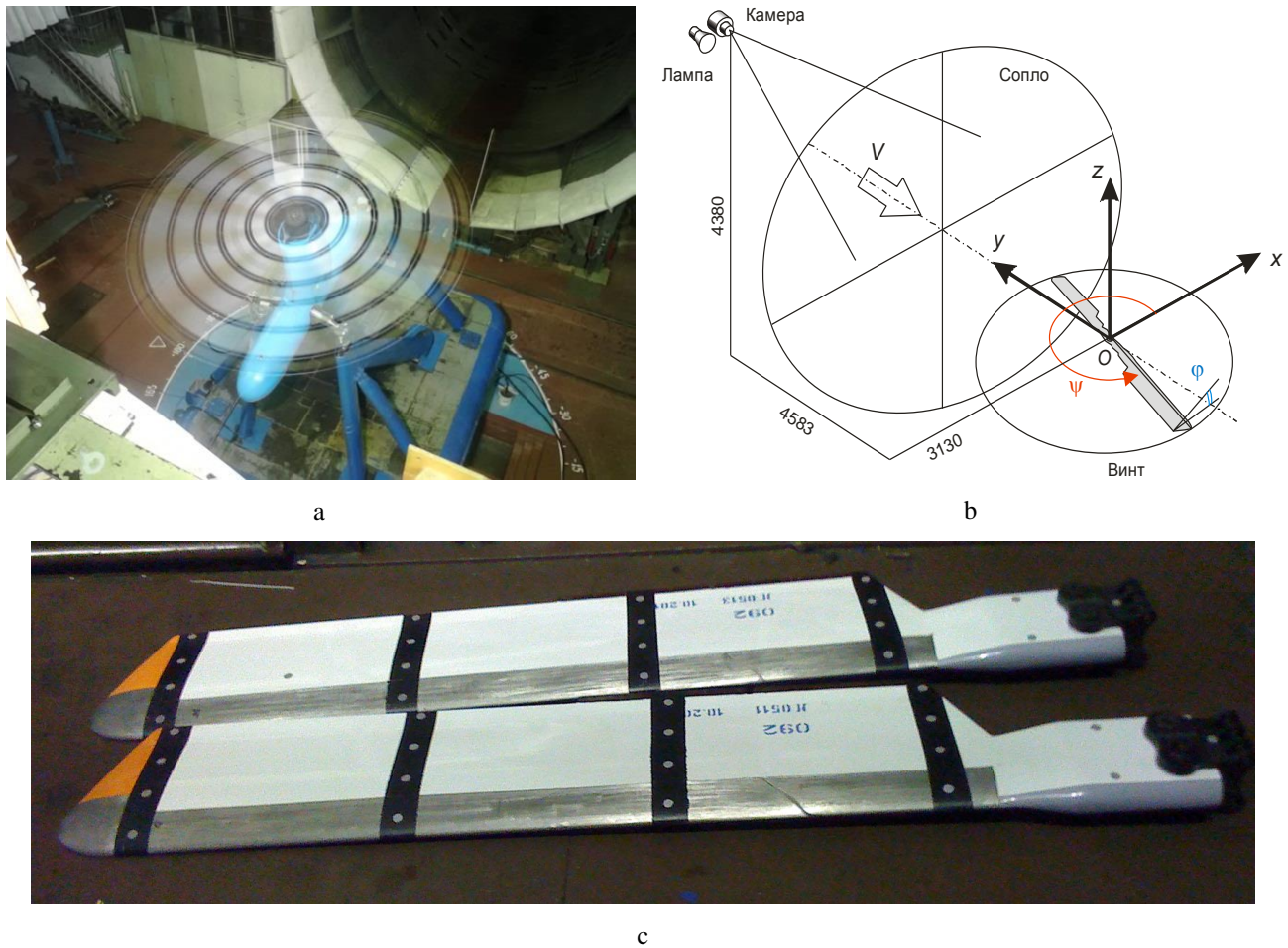


Fig. 14 Photo of the experimental setup in the wind tunnel T-104 (a), measurement scheme (b) and view of blades 1 and 2 with applied retroreflective markers (c)

As a result, the method with location of recording camera motionlessly fixed aside from the investigated object was applied. The complex parametric hypothesis of blade motion including a circular motion in the plane of rotation, flapping in the plane perpendicular to the plane of rotation and rotational motion associated with propeller pitch control was taken as apriori information. Parametric model of blade motion was set as a combination of the following movements:

- blade deformation in the vertical plane defined by the third degree polynomial:

$$\Delta z = c_0 + c_1 \cdot \rho + c_2 \cdot \rho^2 + c_3 \cdot \rho^3$$

where $\rho = \frac{r - r_{\text{ш}}}{R - r_{\text{ш}}}$, r is current coordinate along the longitudinal axis of the blade, $r_{\text{ш}}$ – radius of the

horizontal hinge, R – radius of the blade;

- blade setting angle φ around the longitudinal axis

$$\begin{cases} y_{\varphi} = y' \cdot \cos \varphi - (z + \Delta z) \sin \varphi, \\ z_{\varphi} = y' \cdot \sin \varphi + (z + \Delta z) \cos \varphi, \end{cases}$$

where y' is coordinate along a chord of the blade from its axis in the direction of the front edge;

- total rotation of rotor along azimuth on angle ψ

$$\begin{cases} x = y_{\varphi} \cdot \cos \psi - x \cdot \sin \psi, \\ y = y_{\varphi} \cdot \sin \psi + x \cdot \cos \psi, \\ z = z_{\varphi}, \end{cases}$$

where x, y, z are coordinates of points on blade surface in measurements coordinate system. Fig. 14 b shows the arrangement scheme of the measurements system and the coordinate system with coordinate axes orientation and some linear dimensions measured instrumentally.

Tests were carried out on the helicopter unit VP-6 in wind tunnel T-104 in TsAGI. The rotor contained two blades. On each blade four sections were assigned and four specific retroreflective markers with diameter of 14 mm were glued in each section (Fig. 14 c). Additionally, the same markers were applied on the fasteners elements, blade sleeves and on the rotor shaft. Recording digital camera with a resolution of 1392×1040 pixels was installed and rigidly fixed on the top of nozzle exit section of wind tunnel. Measurements were carried out with a rotor rate of 380 rpm at different modes by rotor thrust from 0 to 110 kgf and flow velocity from 0 to 50 m/s. In each mode from 15 to 20 images were recorded.

Measurement results contained all the parameters of motion, including:

- c_0, \dots, c_3 parameters of elastic line shape of the blade in vertical plane, which are used to calculate shape the elastic line shape of the blade. Fig. 15 represents the examples of elastic line shape of two blades at the flow velocity 30 m/s, rotating rate 380 rpm and rotor thrust 90 kgf;
- the motion trajectory of the blades tip in the vertical plane. The graph of the motion of one of the blades tip is shown in Fig. 16. Continuous line data are the results of approximation with Fourier series of the second order.

Parameters obtained made it possible to construct a mathematical reversion model of motion of each blade. Comparing this model with the results of individual measurements of point coordinates, one can obtain a picture of local deformations. Fig. 17 represents an example of distribution patterns of local bending and twist deformations of blade 1 at the considered mode of rotation.

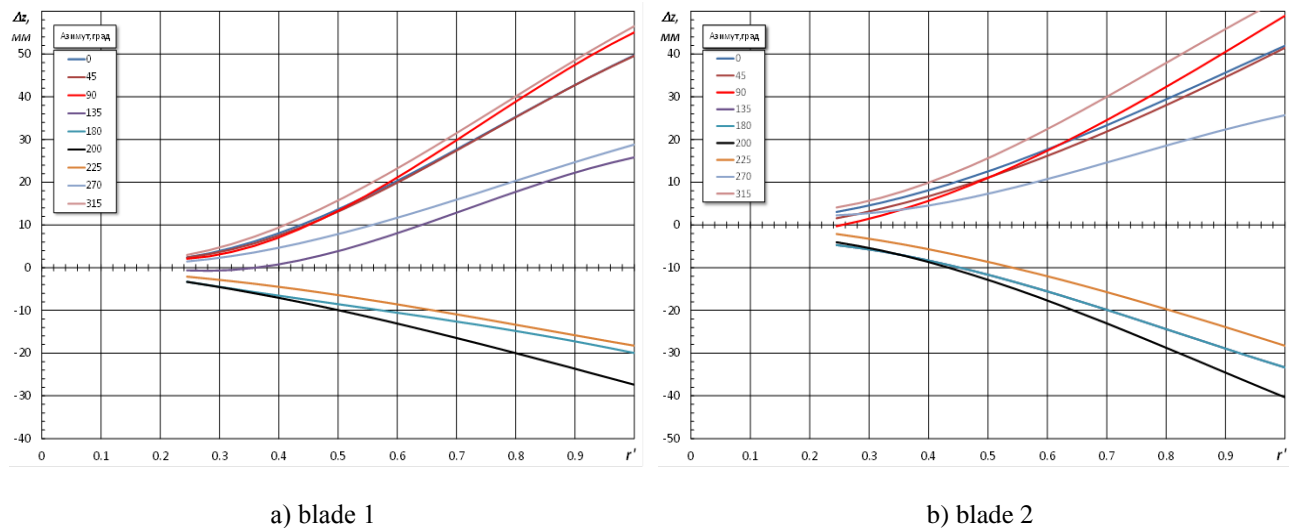


Fig. 15 Elastic line shape of two blades in the vertical plane

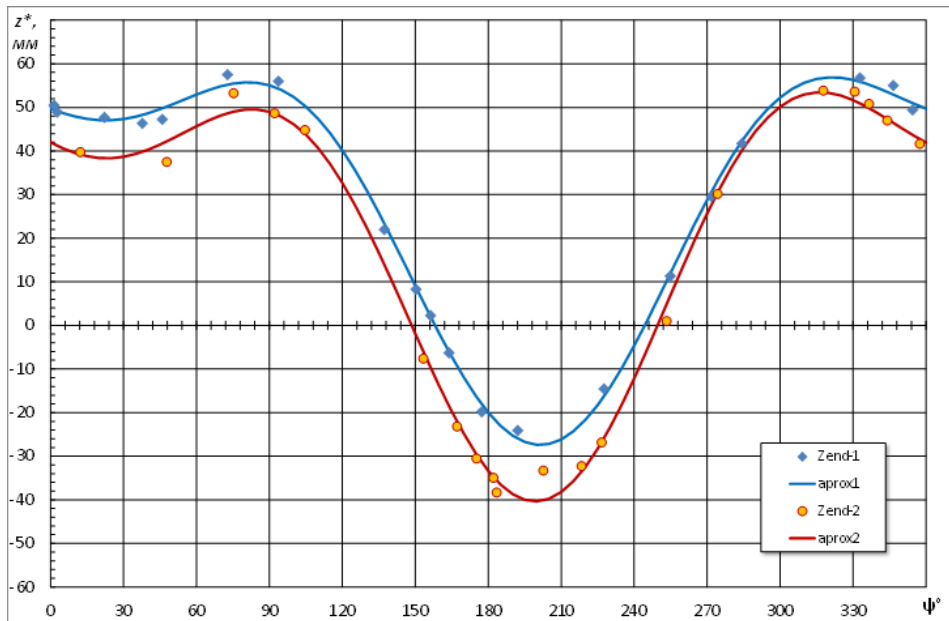


Fig. 16 The trajectory of azimuthal motion of the two blades tips

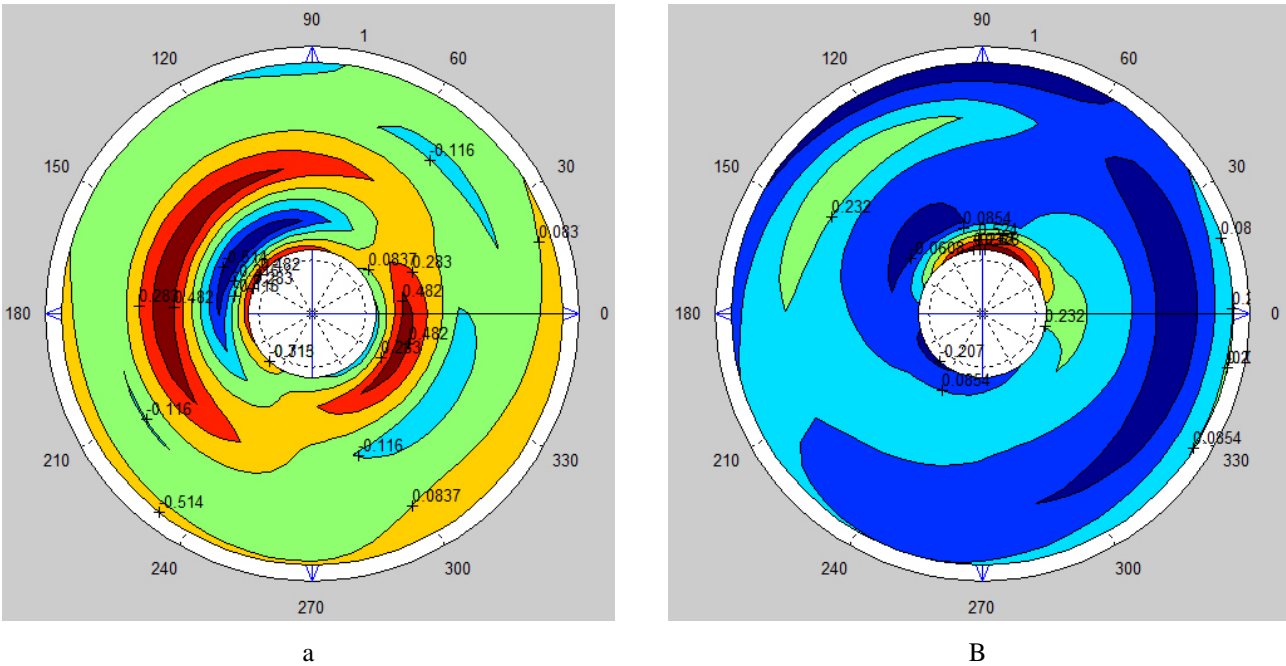


Fig. 17 Pictures of the distribution of local bending (a) and twist (b) deformations of blade

9 Conclusion

1. A conception of videogrammetry with using one digital camera only is being developed. In this method the uncertainty of coordinates recovering problem is solved by the use of apriori information about the investigated object.
2. It is proposed to formulate prior information in the form of mathematical parametric hypothesis and complement the system of equations of the operating characteristics by it.
3. Calibration of the measurement system is recommended to carry out in two stages. The first stage involves the definition of parameters of interior orientation with the greatest possible precision in laboratory conditions. The second stage involves the definition of exterior orientation parameters in a wind tunnel or experimental facility.
4. It is shown in practice that, in the conditions of aerodynamic experiment measurement error is about 0.1 mm/m.
5. The developed VGM methods serve as a good tool for non-contact measurement of geometric parameters of motion and deformation of models and structure elements in experimental aerodynamics. Given here examples demonstrate possibilities of application of VGM methods for the research of position and deformation of model in wind tunnel flow, and also for deformation measurements of the rotating machinery elements.

10 References

- [1] Kulesh V P (2004) Non-contact measurements of geometrical shape parameters, motion and deformation of objects in experimental aerodynamics. *Sensors and systems*, № 3, pp 22-27.
- [2] Kulesh V P, Fonov S D (1998) Measurement of parameters of motion and deformation of aircraft model in a wind tunnel by videogrammetry method. *Scientific notes of TsAGI*, v.XXIX, №1-2. pp 165-176.
- [3] Kulesh V P (2014) Measurements of deformation of adaptive nose wing part in wind tunnel flow using videogrammetry method. *Scientific notes of TsAGI*, v. XLV, № 6, pp 100-109.
- [4] Bosnyakov S, Bykov A, Coulech V, et.al (1997) Blade deformation and PSP measurements on the large scale rotor by video metric system. *ICIASF Record, International Congress on Instrumentation in Aerospace Simulation Facilities*, pp 95.
- [5] Bosnyakov S, Kulesh V, Morozov A, Tarasov N, Fonov S (1999) Videogrammetric system for study of movement and deformation of real-scaled helicopter rotor blades. *Proceedings of SPIE, The International Society for Optical Engineering*, 3516 (I) , pp 196.
- [6] Inshakov S I, Kulesh V P, Mosharov V E, Radchenko V N (2013) Videogrammetry method of non-contact measurements of instantaneous deformation of aerial rotating propeller blades. *Scientific notes of TsAGI*, v. XLIV, № 4, pp 72-79.